

**Supplementary Information for:**

**Boosting the antimicrobial action of vancomycin  
formulated in shellac nanoparticles of dual-  
surface functionality**

**Saba S.M. Al-Obaidy,<sup>a,b</sup> Ahmed F. Halbus<sup>a,b</sup> Gillian M. Greenway<sup>a</sup> and Vesselin N. Paunov<sup>\*,a</sup>**

<sup>a</sup> *Department of Chemistry and Biochemistry, University of Hull, Hull, HU67RX, UK.*

<sup>b</sup> *Department of Chemistry, College of Science, University of Babylon, Hilla, Iraq.*

*\*Corresponding author: Email: [V.N.Paunov@hull.ac.uk](mailto:V.N.Paunov@hull.ac.uk)*

(Journal of Materials Chemistry B 2019)

## Stability of the shellac NPs

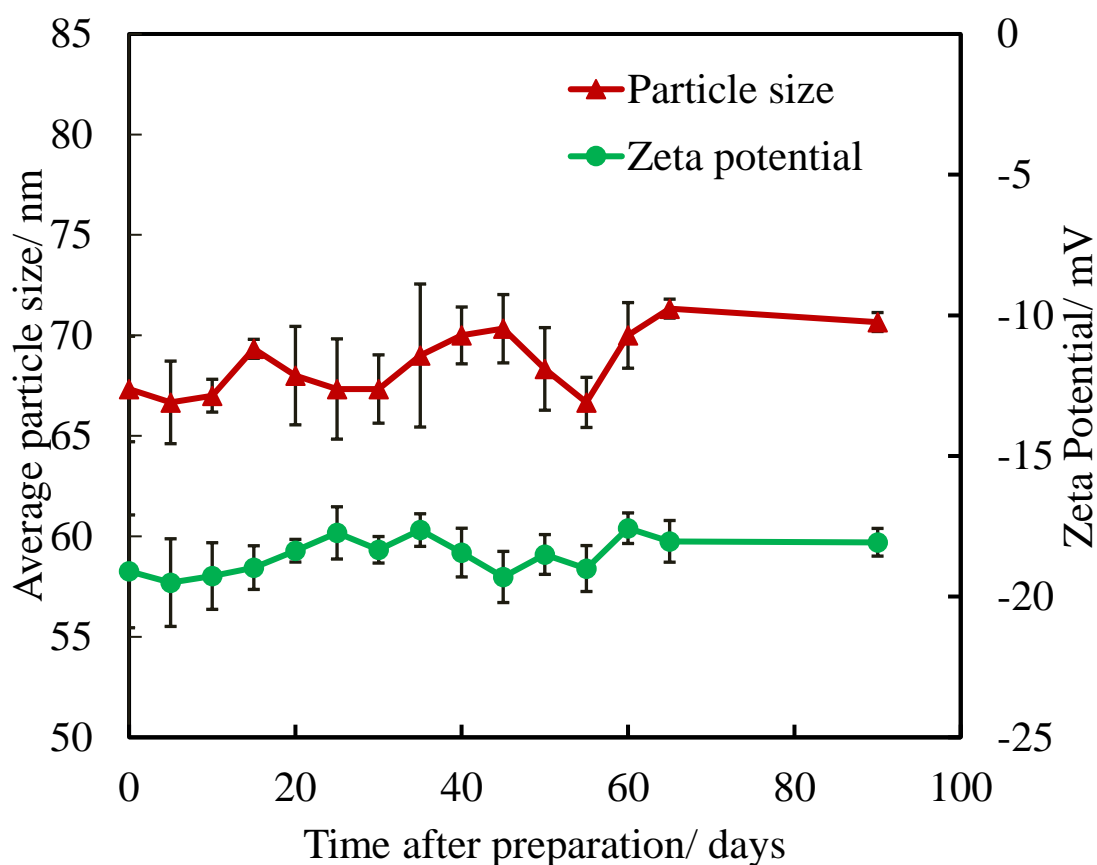


Figure S1. The average particle hydrodynamic diameter and the zeta-potential of shellac NPs at different time using DLS technique. The data are averaged from 3 samples.

In order to investigate shellac NPs storage condition, the size distribution and zeta potential of the nanoparticles were measured as a function of time, up to 90 days in deionised water. Figure S2 (ESI) shows the particle size and zeta-potential of shellac NPs and as it can be seen that shellac NPs are stable within period last more than three months with hydrodynamic diameter of around 68 nm and surface charge of  $-18 \pm 5$  mV. This shows that the shellac NPs can be stored for a long time without aggregation and used to encapsulate actives with long shelf life.

## TEM images and size distribution of shellac NPs stabilised by P407

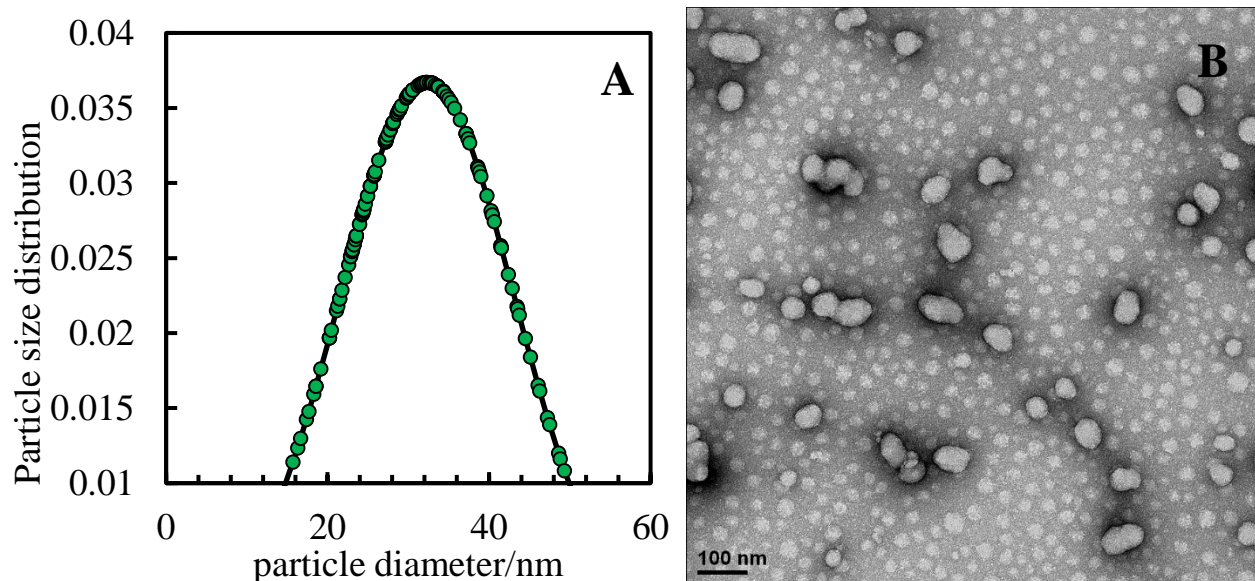


Figure S2. (A) The shellac NPs size distribution measured for a suspension consisting of 0.25 wt. % shellac with 0.2 wt. % P407 in deionised water measured from series of TEM images. (A): Typical TEM image of shellac NPs, after being negatively stained with 1% uranyl acetate.

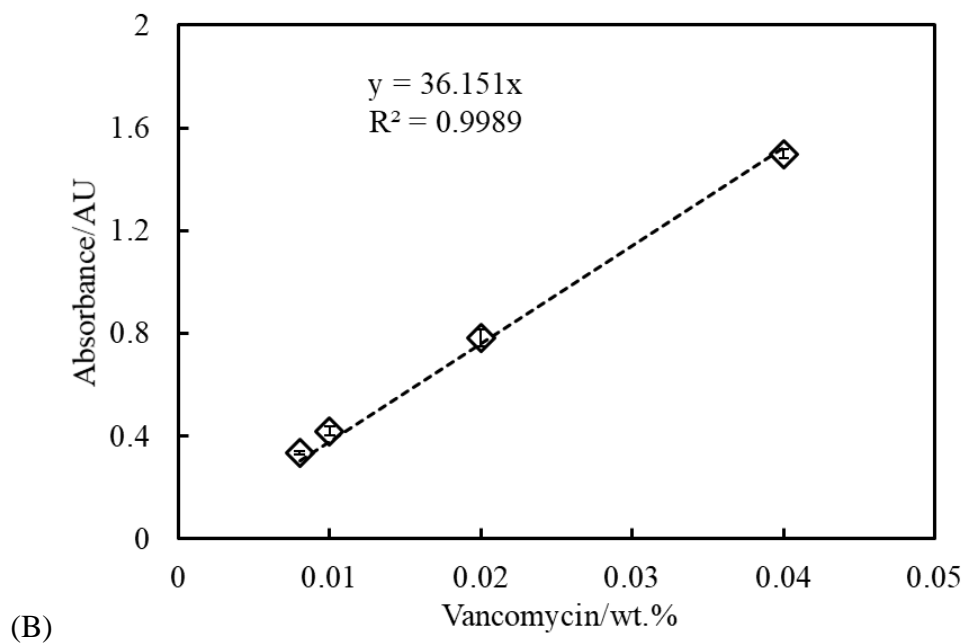
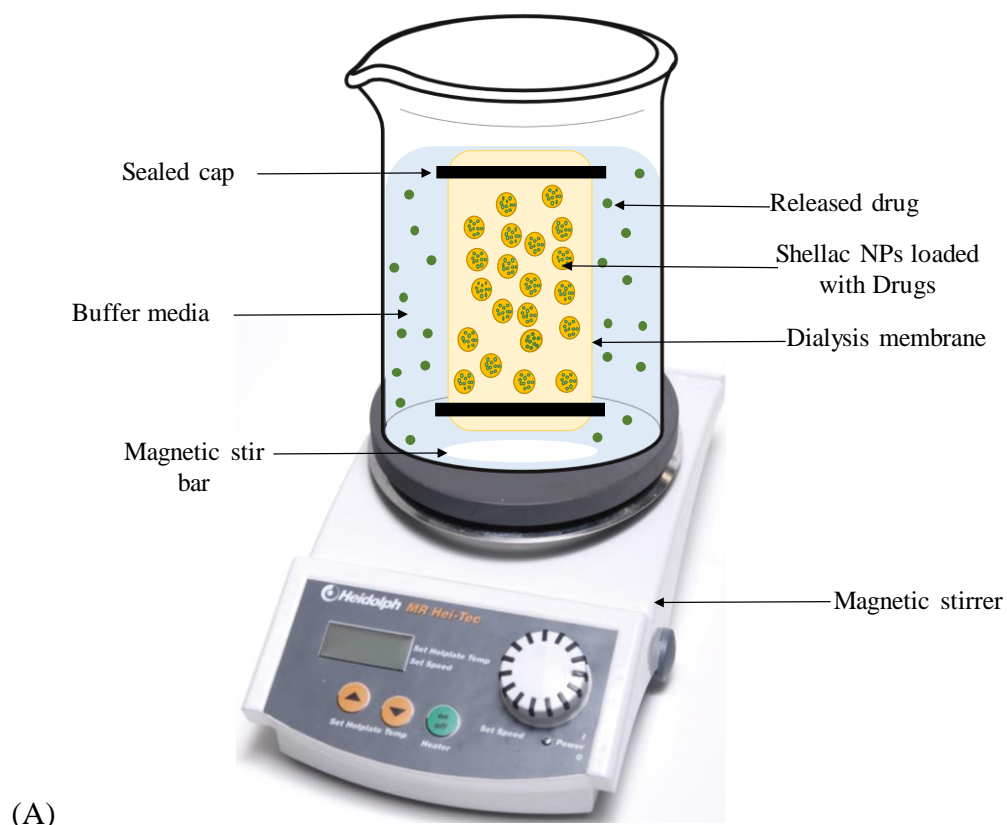


Figure S3. (A) Schematic diagram represents the dialysis process using dialysis bag with pore size of 2.5 nm to allow the drug to be released without the nanocarriers crossing the membrane. (B) The standard curve of different concentrations of vancomycin hydrochloride at wavelength 280 nm.

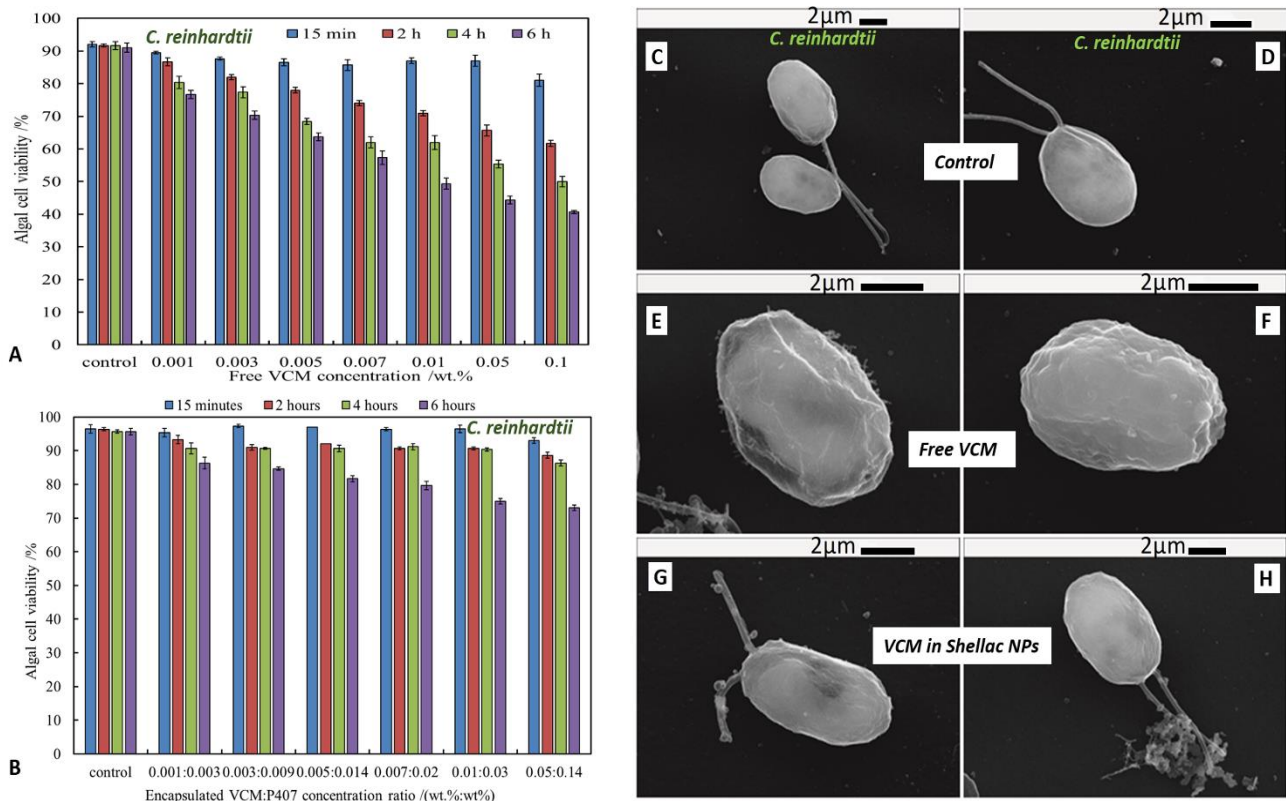


Figure S4. The viability of *C. reinhardtii* upon incubation at pH 5.5 with aqueous solutions of different concentrations of (A) free VCM and (B) VCM-loaded shellac NPs (non-coated with ODTAB) at room temperature up to 6 hours incubation time at pH 5.5. (C)-(H) SEM images of *C. reinhardtii* whereby (C)-(D) represent the control sample of the microalgae cells. (E)-(F) *C. reinhardtii* incubated with 0.01 wt. % free VCM after 4 hours incubation, (G)-(F) *C. reinhardtii* incubated with 0.01 wt. % VCM-loaded in shellac NPs for 4 hours. Note that the free VCM is more effective anti-algal agent than the non-coated shellac NPs with the same concentration of loaded VCM.

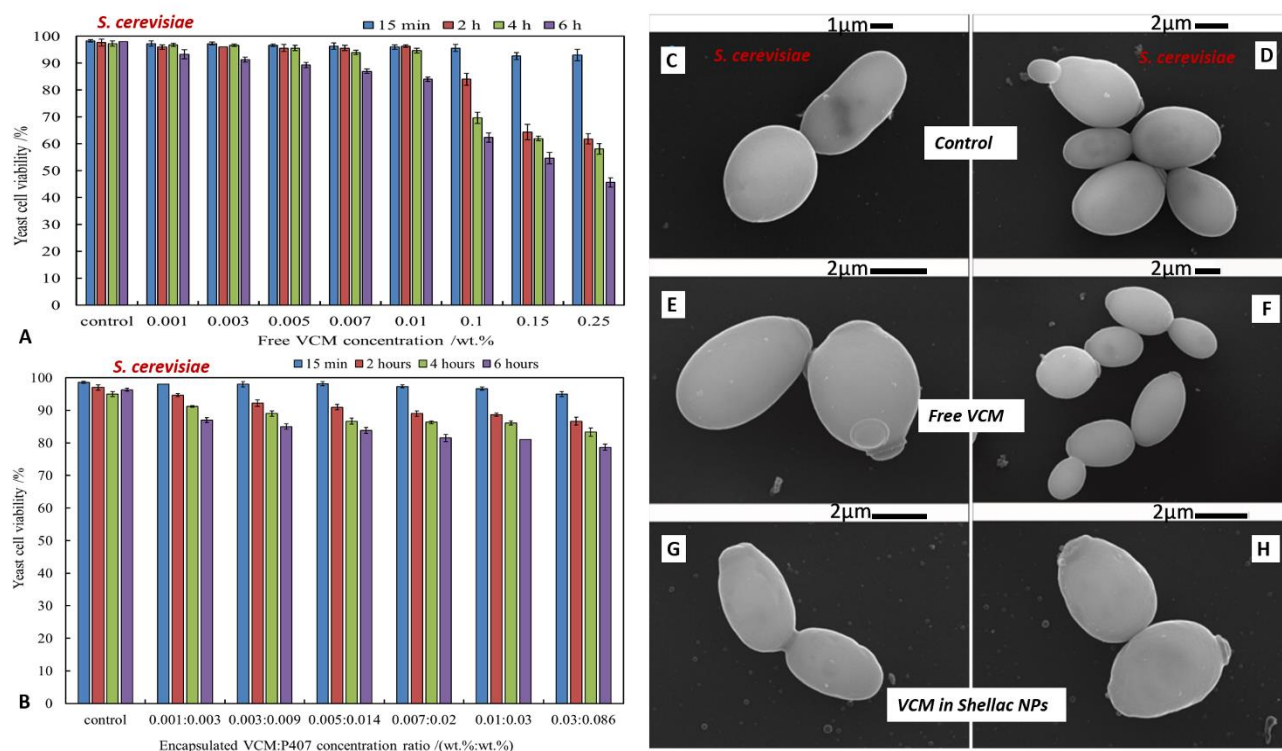


Figure S5. The viability of *S. cerevisiae* upon incubation at pH 5.5 with aqueous solutions of different concentrations of (A) free VCM and (B) VCM-loaded shellac NPs (non-coated with ODTAB) at room temperature up to 6 hours incubation time at pH 5.5. (C)-(H) SEM images of *S. cerevisiae* whereby (C)-(D) represent the control sample. (E)-(F) *S. cerevisiae* cells incubated with 0.01 wt. % free VCM after 4 hours incubation, (G)-(F) *S. cerevisiae* incubated with 0.01 wt. % VCM-loaded in shellac NPs for 4 hours. Note that the free VCM is more effective anti-yeast agent than the non-coated shellac NPs with the same concentration of loaded VCM.

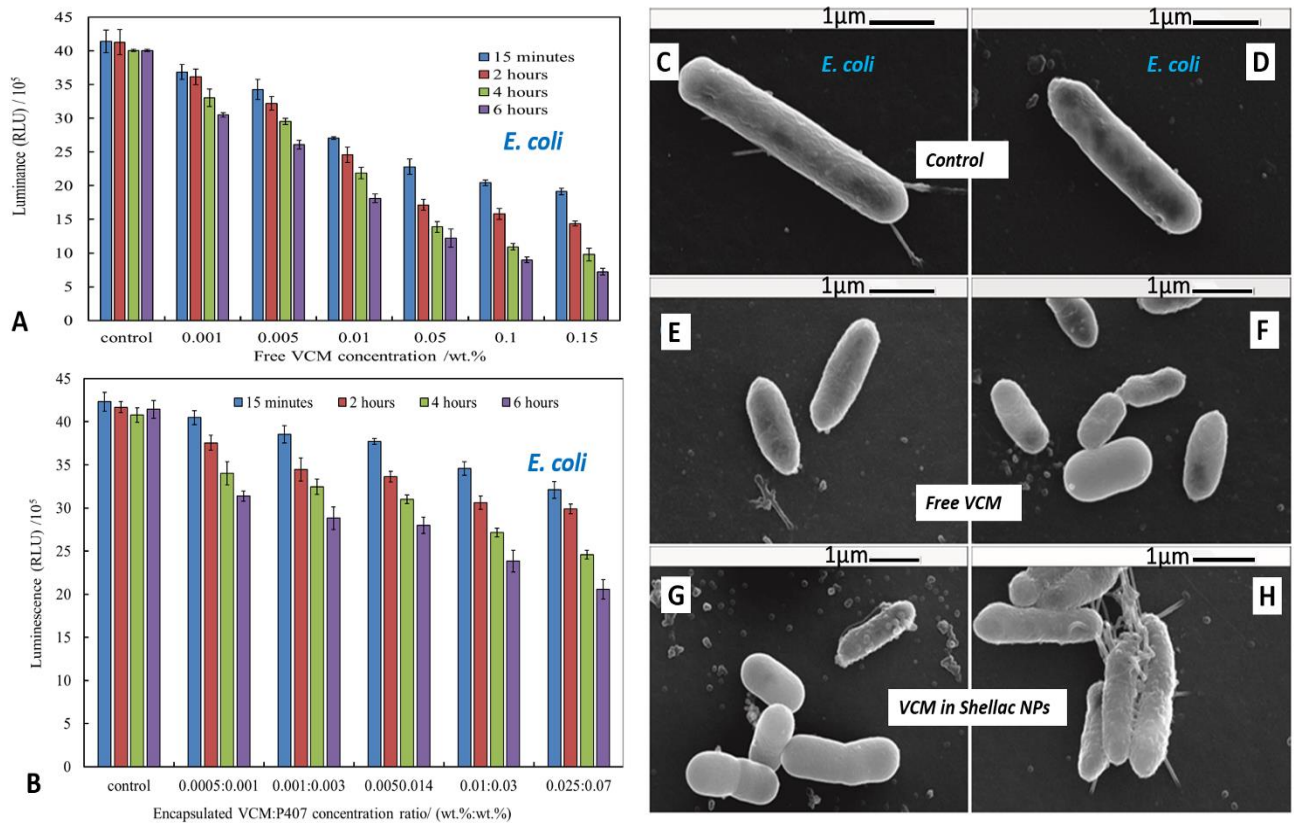


Figure S6. The viability of *E. coli* upon incubation at pH 5.5 with aqueous solutions of different concentrations of (A) free VCM and (B) VCM-loaded shellac NPs (non-coated with ODTAB) at room temperature up to 6 hours incubation time at pH 5.5. (C)-(H) SEM images of *E. coli* whereby (C)-(D) represent the control sample of the microalgae cells. (E)-(F) *E. coli* incubated with 0.01 wt. % free VCM after 4 hours incubation, (G)-(F) *E. coli* incubated with 0.01 wt. % VCM-loaded in shellac NPs for 4 hours. Note that the free VCM is more effective anti-bacterial agent than the non-coated shellac NPs with the same concentration of loaded VCM.

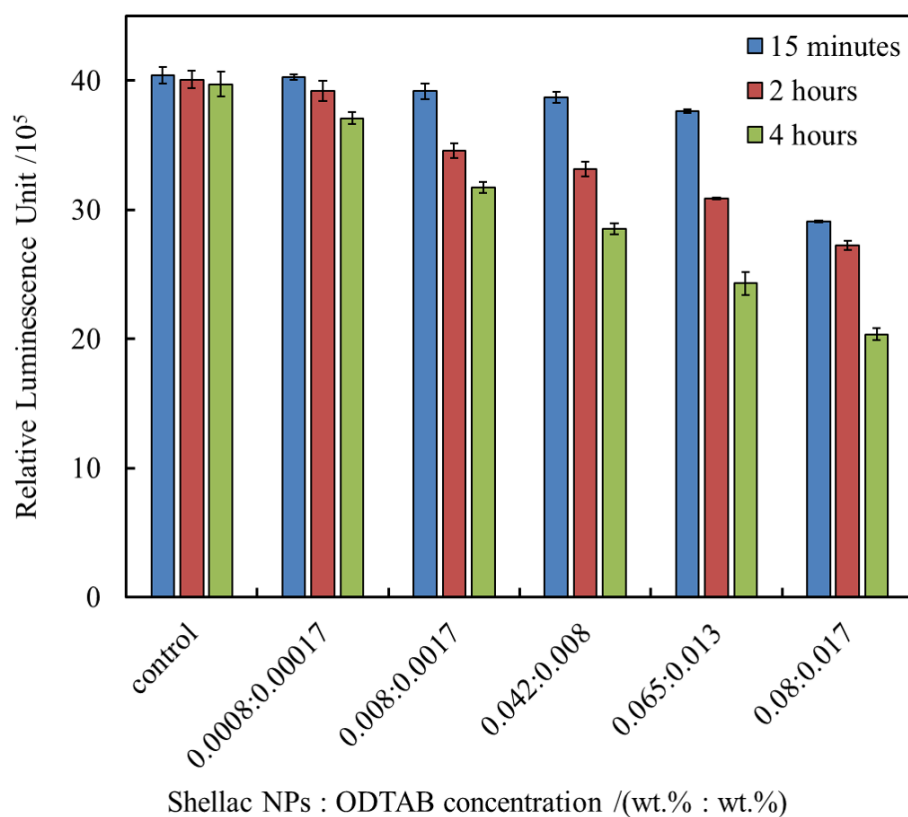


Figure S7. The cytotoxic effect of non-loaded ODTAB-coated shellac NPs of different concentrations on *E. coli* for several different incubation times at room temperature. The shellac NPs were not loaded with VCM. The ratio of shellac:ODTAB in the NPs is fixed to 5:1. The x-axis shows the variation of the shellac and ODTAB concentrations for these experiments.



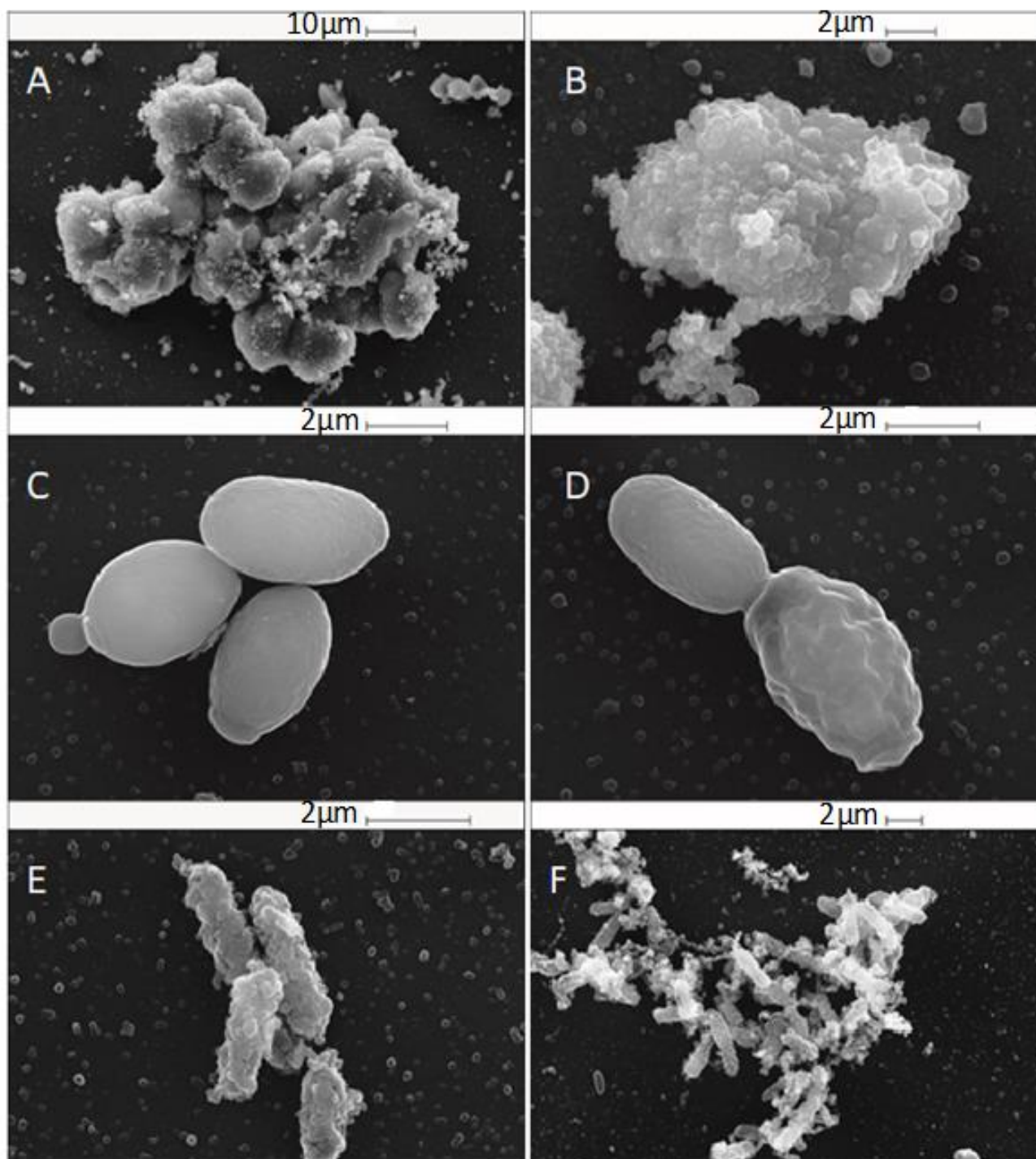


Figure S8: SEM images of microorganisms cells with 0.025 wt.% ODTAB-coated 0.125 wt.% shellac NPs after 4 hour incubation at pH 5.5. (A, B) *C. reinhardtii* cells, (C, D) yeast cells, and (E,F) *E. coli* cells. The shellac NPs were not loaded with VCM.

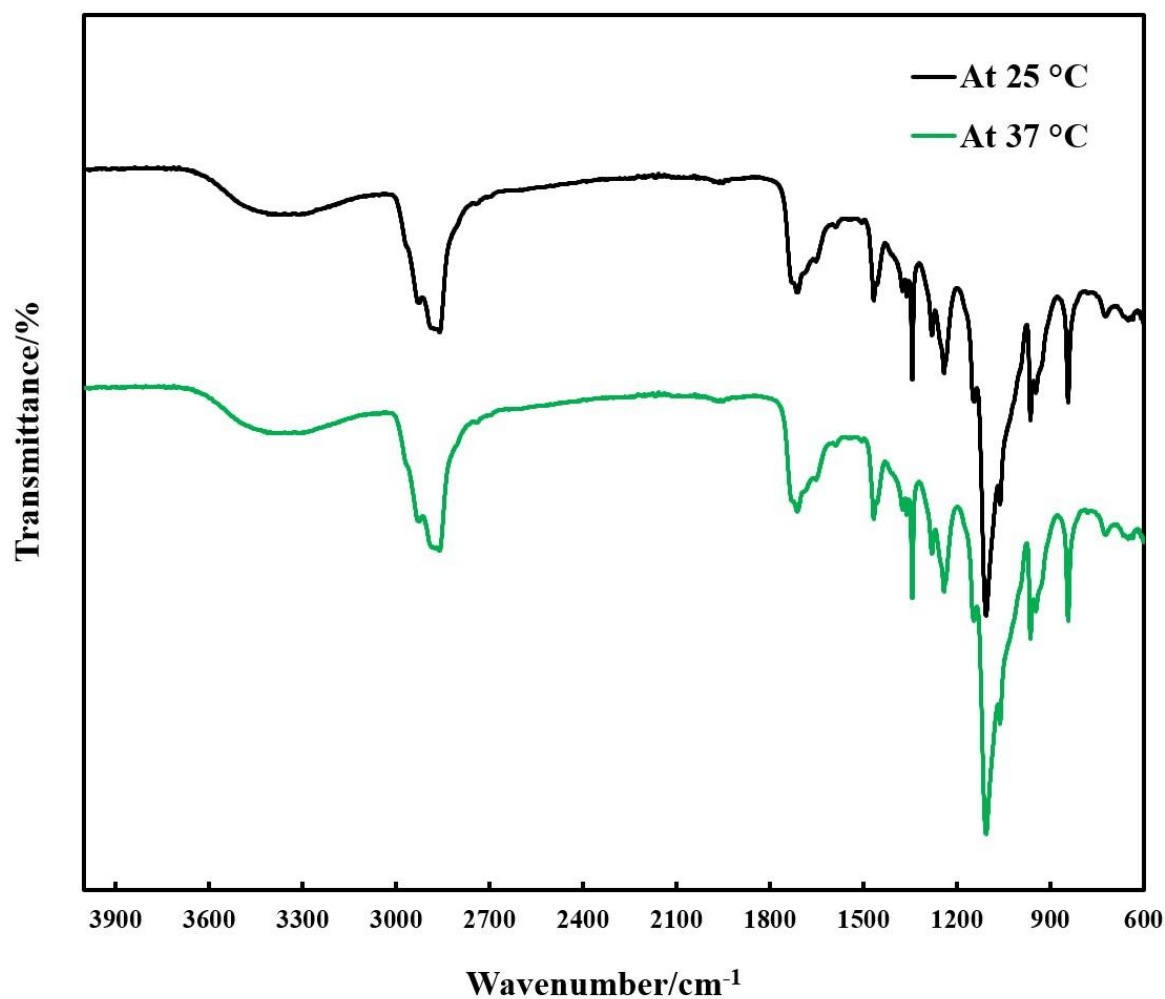


Figure S9. Thermal stability of the VCM-loaded shellac nanocarrier assessed by FTIR spectrum after incubation of a sample of the nanocarrier at 37 °C for up to 2 hours compared with the control sample kept at 25 °C. Note that the FTIR spectra are identical, i.e. the incubation at 37 °C does not change the VCM or the shellac nanocarrier.